LPV-H_∞ Control with Optimal Weighting Functions Selection by Nature-Inspired Algorithms, Applied to an Inverted Pendulum on Cart

SEIF-EL-ISLAM HASSENI[1*], LATIFA ABDOU[2]

[1] LMSE Laboratory, Electrical Engineering Department, University of Biskra, Algeria.
[2] LI3CUB Laboratory, Electrical Engineering Department, University of Biskra, Algeria.
[*] Corresponding author, e-mail: seif.hasseni@univ-biskra.dz

Abstract: -In this paper, the robust stabilization and control of an inverted pendulum on cart is investigated; the robustness is guaranteed against the external inputs; disturbances and measurement noises, and parametric uncertainties. The contribution is based on creating this nonlinear system as a Linear Parameter Varying System (LPV) to allow the applying of robust LPV techniques possible. In addition, one of the more constraints is the selection of the weighting functions that represent the desired performance; in this work we used two approaches of optimization nature-inspired algorithms; Genetic Algorithms (GA) and Evolutionary Strategies (ES) to find the weighting functions' parameters, with guarantee the robustness against external signals and uncertainties. Last more point, the represented underactuation constraint of the selected vehicle; we extend the robust stabilization by considering the both of degrees of freedom; the rotational and the translational. The controllers we get are robust against the external signals and uncertainties, and with the nonlinear range of angles as initial conditions.

Keywords: -Inverted Pendulum on cart, Robust Control, Underactuated Systems, Nature-Inspired Algorithms, Linear Parameter Varying Systems, H_∞.

1 Introduction

The H_∞ control is one of efficient control approaches on the robustness problem; where the objective is to minimize the gain between the external input signals and the so-called output signals [1] basically developed for the Linear Time Invariant systems (LTI systems). In recent years the Linear Parameter Varying systems (LPV systems) have been interested by researchers, and several works have investigated the control synthesis and stability analysis of the LPV systems [2],[3],[4], because of their main advantage to allow the modeling a systems that basically depend on time varying parameters or to approximate the nonlinear systems. Alternatively to divide the nonlinear system in a set of LTI systems according their operating points, the LPV system is developed by considered the nonlinearities as varying parameters, it is called here a quasi-LPV system [5], [6], which is what we are studying in this paper.

There are common approaches to develop the LPV systems from their origin, nonlinear. First, the polytopic approach; the parameters are used at each vertex in the polytope, as main disadvantage of this approach is that it requires an exponential number of controllers, therefore, solving a large numbers of Linear Matrices Inequalities (LMI), the compute effort is expensive [7], [8], [9]. Second, gridding linearization; with this approach, there are simple controllers to implement, but, infinity elements because the descritization on the parameters space is not well defined [10]. Third and last one, the LPV system with Linear Fractional Transformation (LFT), it is common on separating the uncertainties from the nominal model in robust control, the same structure we will get with the varying parameters, the main advantage of this approach is that we solve a minimal LMI to design a single controller, this last has a self-scheduled structure around the parameters [11].

The presented paper aims to investigate the design of a robust controller for an inverted pendulum on cart by using an LPV technique. The inverted pendulum is a classical benchmark, it has two Degrees Of Freedom (DOF); the translational movement of the cart (denote x) and the angular position of the pendulum (denote θ), when its motion is controlled by a single horizontal force which moves the cart forward or backward. In previous work [12], we eliminated the translational DOF by taking a reduced model; the model was presented by two states (θ, $\dot{\theta}$), the objective was stabilize the pendulum in null angle with robustness against disturbance and uncertainties.

The novelty in this work is presented within these three points; include the friction effect and consider the velocity as a state (a), getting optimal weighting functions (b) and both of the 2 DOF (θ and x) are stabilized on the same time (c).

a) The same technique of the controller design (LFT-based LPV H_∞) is applied here, but unlike [12], we manipulate with the complete model, considering the friction effect, that means that the translational velocity has been included as a state. We note here that we don't consider the translational position (x) as a state; it isn't necessary to measure or estimate the position of a personal pendulum vehicle (i.e. segway) when the objective is to stabilize it because the rider can move it by inclining himself.

b) One of the problems we face in the design of H_∞ controller is the weighting functions selection, which depends on experimental skills, many researches were cared about this issue [1], [13], [14], but, there is no general methodology to select the weighting functions. This problem is more shown on complex systems when the performance specification is not (or is difficult to) defined; when we impose such, optimal, desired performance presented by the weighting functions, the H_∞ controller design process maybe failed to find a suitable controller for such performance, the solution is that we have to demean the performance specification. Nature inspired stochastic optimization tools have used in many researches to get the optimal weighting functions parameters with existing H_∞ controller, for LTI system [15], and for a polytopic-LPV system [16], [17]. These tools are more required in the multi-objective problem, which is very common on controller designing process. In order to get the optimal weighting functions' parameters, we use in this paper two evolutionary algorithms; first, the Genetic Algorithm (GA) which is based on Darwinian evolution, is created by Holland [18], second, the Evolutionary Strategies (ES), the first evolutionary algorithm, which is based on biological evolution, is created by Ingo Rechenberg [19].

c) With 2DOF (x and θ) and just one input (Force), the inverted pendulum is an Underactuated Mechanical System (UMS), previously, the objective is to stabilize the pendulum to its origin angle whatever the linear velocity of the vehicle (although it is constant) [12], but now, the objective is to stabilize it by considering the 2DOF, without adding any new actuators and settle of just one input.

The outline of the paper is as fellows; in Section 2, we introduce the proposed vehicle to control, the inverted pendulum in cart; its model and its equivalent LFT-LPV representation. In Section 3, we will show the selected evolutionary algorithms, GA and ES, and the characteristics for such technique we use. In Section 4, after we get the closed loop system, including the disturbance, the measurement noise and the weighting functions, we will apply the optimization process to get the optimal weighting functions parameters, we notice here that we consider the angle as the only output. The underactuated degrees of freedom are taken into account in Section 5, and we will show the ultimate simulation results of stabilizing the both degrees of freedom. Finally, our conclusion is presented in Section 6.

2 The Inverted Pendulum on Cart

In this paper, we consider a vehicle called personal pendulum vehicle [20] (Fig.1). The personal pendulum vehicle is an inverted pendulum with two wheels, the rider is presented the pendulum who guides it moving forward or backward by inclining himself.

Fig.1 General view of the personal pendulum vehicle

The inverted pendulum in cart model is a benchmark for many autonomous vehicles [21] which is a vehicle has two degrees of freedom, one is relating on the angular coordinate (θ) and other is relating on translational coordinate (x), but the applied only input is the linear thrust force (F). The control objective is to stabilize the pendulum in the null angle, whatever the initial angle (Fig.2). In the next subsection we will show its nonlinear model.

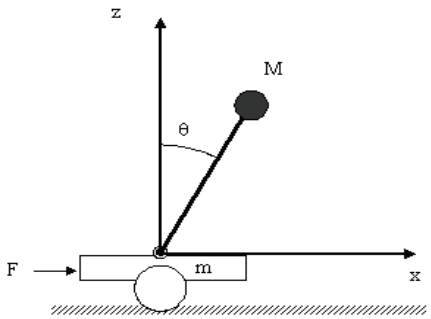

Fig.2 Geometric scheme of an inverted pendulum on cart

2.1 The mathematic model of the inverted pendulum on cart

A dynamic model of any mechanical system can be derived from Lagrange-Euler formulation, so, we can describe the dynamic model of any mechanical system as follows:

$$M(q)\ddot{q} + C(q,\dot{q})\dot{q} + G(q) = u \quad (1)$$

Where; q is degree of freedom coordinate, $\dot{q}$ and $\ddot{q}$ are its first and second derivative, $M(q)$ is the symmetric definite positive inertia matrix, the term $C(q,\dot{q})$ is the Centrifugal and Coriolis matrix, the term $G(q)$ are the gravitational torques and u is the inputs.

The dynamical model of the considered system, the inverted pendulum, is presented in next expression [22],[20]:

$$\begin{bmatrix} M+m & Ml\cos(\theta) \\ Ml\cos\theta & Ml^2 \end{bmatrix}\begin{bmatrix} \ddot{x} \\ \ddot{\theta} \end{bmatrix} + \begin{bmatrix} b & -Ml\,sin(\theta)\dot{\theta} \\ 0 & 0 \end{bmatrix}\begin{bmatrix} \dot{x} \\ \dot{\theta} \end{bmatrix} + \begin{bmatrix} 0 \\ -Mgl\sin\theta \end{bmatrix} = \begin{bmatrix} F \\ 0 \end{bmatrix} \quad (2)$$

Where, m is the mass of the cart, M is the pendulum mass, presents here the mass of the rider who guides the vehicle, l is the pendulum length, g is the gravity constant, b is the linear friction force coefficient and F is the linear force applied in the vehicle. Table 1 presents the nominal values.

Table 1 Nominal parameters of the vehicle

Parameter	Description	Value	Unit
m	Cart's mass	35	Kg
M	Pendulum's mass	70	Kg
l	Pendulum's arm length	1	m
g	Gravity constant	9.8	$m.s^{-2}$
b	Friction coefficient	40	$N.s.m^{-1}$

The objective of this research is the robust control of a nonlinear system by the robust LPV, so, we will create the nonlinear model of the inverted pendulum (2) as an LPV with LFT representation in the next subsection.

2.2 The LFT-LPV representation of the inverted pendulum on cart

We have to present our system's nonlinear model (2) as an LPV. The general state space of an LPV system is as follows:

$$\begin{cases} \dot{x} = A(\rho)x + B(\rho)u \\ y = C(\rho)x + D(\rho)u \end{cases} \quad (3)$$

Where; x is the state vector, u, the input vector, A, B, C, and D are the dynamic matrices, they are depending on the varying parameters ρ.

As we mentioned previously, there are different presentations of an LPV system; polytopic, gridding and LFT. We use the last one to present the inverted pendulum model based on many advantages; i.e. single scheduled controller.

We have to notice that the controller has the same representation of the system.

We extract the two equations from (2):

$$\begin{cases} (M+m)\ddot{x} + Ml\cos(\theta)\,\ddot{\theta} + b\dot{x} - Ml\sin(\theta)\dot{\theta}^2 = F \\ Ml\cos(\theta)\,\ddot{x} + Ml^2\ddot{\theta} - Mgl\sin(\theta) = 0 \end{cases} \quad (4)$$

We face on the issue that the term $(Ml\sin(\theta)\dot{\theta}^2)$ makes the model difficult to apply the chosen LPV technique. We have exceeded this problem by changing the generated signal by the controller, the new dynamic model is:

$$\begin{cases} (M+m)\ddot{x} + Ml\cos(\theta)\,\ddot{\theta} + b\dot{x} = u \\ Ml\cos(\theta)\,\ddot{x} + Ml^2\ddot{\theta} - Mgl\sin(\theta) = 0 \end{cases} \quad (5)$$

Where:

$$u = F + Ml \sin(\theta)\dot{\theta}^2 \quad (6)$$

By replacing one equation of (5) on the other, we take the nonlinearities as varying parameters. After some changes we extract the LFT-LPV state space (7) and its structure (Fig. 3):

$$\begin{bmatrix} \dot{x} \\ z_\rho \\ y \end{bmatrix} = \begin{bmatrix} \mathcal{A} & \mathcal{B}_\rho & \mathcal{B}_1 \\ \mathcal{C}_\rho & \mathcal{D}_{\rho\rho} & \mathcal{D}_{\rho 1} \\ \mathcal{C}_1 & \mathcal{D}_{1\rho} & \mathcal{D}_{11} \end{bmatrix} . \begin{bmatrix} x \\ w_\rho \\ u \end{bmatrix} \quad (7)$$
$$w_\rho = \Theta\, z_\rho$$

Where: x is the states' vector, $x = [\theta \quad \dot{\theta} \quad \dot{x}]^T$, u is the input, where is just the force F, z_ρ and w_ρ are the inputs and outputs of the parameters block Θ.

The matrices:

$$\mathcal{A} = \begin{bmatrix} 0 & 1 & 0 \\ \frac{g}{l} & 0 & \frac{b}{(M+m)l} \\ 0 & 0 & \frac{-b}{(M+m)} \end{bmatrix}, \mathcal{B}_\rho = \begin{bmatrix} 0 & 0 & 0 & 0 \\ \frac{g}{l} & \frac{1}{(M+m)l} & 0 & \frac{M}{(M+m)} \\ 0 & 0 & \frac{Ml}{(M+m)} & 0 \end{bmatrix},$$

$$\mathcal{B}_1 = \begin{bmatrix} 0 \\ \frac{-1}{(M+m)} \\ \frac{1}{(M+m)} \end{bmatrix}, \mathcal{C}_\rho = \begin{bmatrix} 1 & 0 & 0 \\ 0 & 0 & b \\ \frac{g}{l} & 0 & \frac{b}{(M+m)l} \\ 0 & 0 & 0 \end{bmatrix}, \mathcal{C}_1 = [1 \quad 0 \quad 0],$$

$$\mathcal{D}_{\rho\rho} = \begin{bmatrix} 0 & 0 & 0 & 0 \\ 0 & 0 & 0 & 0 \\ \frac{g}{l} & \frac{1}{(M+m)l} & 0 & \frac{M}{(M+m)} \\ 0 & 0 & 1 & 0 \end{bmatrix}, \mathcal{D}_{\rho 1} = \begin{bmatrix} 0 \\ -1 \\ \frac{-1}{(M+m)} \\ 0 \end{bmatrix}, \mathcal{D}_{1\rho} = [0 \ 0 \ 0 \ 0],$$

$$\mathcal{D}_{11} = 0, \Theta = \begin{bmatrix} \rho_1 & 0 & 0 & 0 \\ 0 & \rho_2 & 0 & 0 \\ 0 & 0 & \rho_3 & 0 \\ 0 & 0 & 0 & \rho_4 \end{bmatrix} \quad (8)$$

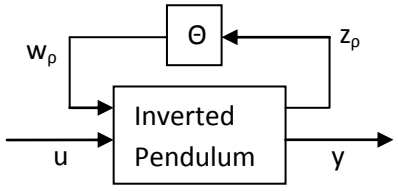

Fig. 3 LFT-LPV scheme of the inverted pendulum

Before designing a controller to stabilize such LPV system, we need to provide the limit bound of each parameter. In our system, all of the parameters; $\rho_1 \ldots \rho_4$ are depended on θ, theoretically $-90° \leq \theta \leq 90°$, but to avoid the non-controllability we have to reduce the bound to $-80° \leq \theta \leq 80°$. Table 2 presents the range of each parameter.

Table 2 The ranges of the varying parameters

Parameter	Description	Min. value	Max. value
$\boldsymbol{\rho_1}$	$\left(\frac{\sin\theta}{\theta}\right) - 1$	-0.3	0
$\boldsymbol{\rho_2}$	$\cos\theta - 1$	-0.83	0
$\boldsymbol{\rho_3}$	$\cos\theta$	0.17	1
$\boldsymbol{\rho_4}$	$cos^2\,\theta$	0.03	1

We notice that, in (7)-(8) we didn't generate the closed loop system yet, just convert the plant (5) to LFT-LPV representation. We need to interconnect the plant with the disturbances and the weighting functions which are the important point on the H_∞ controller design. Our contribution is to select the weighting functions parameters by the nature-inspired algorithms (GA and ES). Next section, we introduce the algorithms that we develop and their characteristics.

3 Nature-inspired Algorithms

The nature-inspired optimization algorithms, especially which called evolutionary algorithms have common tasks on their procedures; selection of initial solutions randomly, evaluate the solutions depending on a fitness function, elimination of the worst solutions and generation of new solutions by the operations; crossover, mutation and selection. Since the implementation of initialization, replacement is not different between these algorithms; the significant difference is the generation of new solutions.

Next, the description of such used algorithm (GA, ES) with its properties and explained by their pseudo-codes.

3.1 Genetic Algorithms

Genetic Algorithm (GA) is one of oldest evolutionary algorithms; it is the most popular EAs in engineering applications. It was developed and created by Holland [18], it is based on the Darwinian evolution of biological systems. Its operators are the biological operators; crossover, mutation and selection, which were applied on each population. The population is divided on individuals, where the best individuals have a chance to survive and transfer their characteristics to the next generation. The individual is called chromosome which presents a solution. In our work we consider the individual as a real-coded solution [23] presented by a vector and the generation is the iteration to generate a new set of solutions. The procedure is as illustrated in *Algorithm 1*:

Algorithm 1 *: Genetic Algorithm*
Initialize a solutions randomly;
While *max_Generation not meet* ***do***
Evaluate each solution;
Rank the solutions;

Recombine_BMW pairs of parents;
Mutate the offspring by p_m;
Replace the worst parents by best offspring;
end while

The operation *Evaluate* is the evaluation according its fitness function, where we need to rank the population according its fitness to perform the Best-Mate-Worst crossover [24], [25], all of the population's individuals are passing on the crossover operation; *Recombine_BMW* is presented by the following expression:

$$\begin{cases} x_i^{t+1} = \alpha . x_i^t + (1-\alpha) . x_j^t \\ x_j^{t+1} = \alpha . x_j^t + (1-\alpha) . x_i^t \end{cases} \quad (9)$$

The operation *Mutate*, is a random mutation which is implemented on a few of offspring (probability of p_m) after the crossover operation. The Gaussian mutation is used as:

$$x_i^{t+1} = x_i^{t+1} + N(0, \sigma) \quad (10)$$

Finally, the operator of the selection, *Replace*, permits to replace the worst individuals of previous generation by the best individuals of the new generation in order to keep the size of population, and pass to the next generation. The parameters are shown at the end of this section in Table 3.

3.2 Evolutionary Strategies

Evolutionary Strategies (ES) is the first proposed evolutionary algorithm, which is based on the biological evolution, commonly used to the optimization problems of continuous systems. Likewise the GA, the ES operators are crossover (combination), mutation and selection [26]. Its main advantage is the self-adaptive control of parameters, especially in the mutation task. ES contains many different strategies; we use here the (μ+λ) strategy [27] with real-coding individuals; in the selection task we took λ individuals from the offspring's population gathered with the best μ individuals from the parent's population, and consider the result as a new generation. Unlike the GA, in the combination (crossover), we don't need here to rank the population, because the combination is achieved randomly between fraction of individuals (we took λ). The procedure is illustrated in *Algorithm 2*:

***Algorithm 2** : Evolution Strategies*
Initialize solutions randomly;
While** max_Generation not meet **do
Generate new solutions;
Recombine pairs of parents;
Mutate the offspring;
Rank the solutions;
Replace new generation (μ+λ);
end while

The crossover task, *Recombine*, is implemented as in the case of the GA (9) by selecting λ parents randomly, with a real-coding of the individuals [23]. The main characteristic of ES is the self-adaptation mutation; so, we propose to use in this work a *log-normal auto-adaptive* mutation in *Mutate* task, as:

$$\sigma^{t+1} = \sigma^t . e^{(\sqrt{n})^{-1} . N(0,1)} \quad (11)$$

$$x_i^{t+1} = x_i^{t+1} + N(0, \sigma^{t+1}) \quad (12)$$

Last operation in each iteration, *Replace*, we take λ individuals of offspring population and the best μ ones of parents' population to transfer them to the next generation. The common parameters are; *max_Generation* which is equal to 20 and *population size* equal to 50. The other parameters are shown in Table 3.

Table 3 Parameteres setting of different algorithms

GA		ES	
Par.	**Val.**	**Par.**	**Val.**
cross.	BMW	p_m	0.3
p_m	0.04	λ	36
α	1/3	μ	14
σ	0.04	σ^0	0.3

4 Controller design and implementation

In this section, the only output we consider is the angle (θ), where the objective is making the pendulum's orientation null without considering the translational DOF.

4.1 The closed loop generation

Before passing to the controller's design phase, we have to generate the closed loop system (plant-controller), including the disturbances and weighting functions, we notice that the controller has the same structure of the plant (Fig. 4).

The LFT-LPV state space of the augmented plant is as follows:

$$\begin{aligned} \dot{x} &= A\,x + B_\rho\, w_\rho + B_1 w + B_2 u \\ z_\rho &= C_\rho x + D_{\rho\rho} w_\rho + D_{\rho 1} w + D_{\rho 2} u \\ z &= C_1 x + D_{1\rho} w_\rho + D_{11} w + D_{12} u \\ y &= C_2 x + D_{2\rho} w_\rho + D_{21} w + D_{22} u \\ w_\rho &= \Theta z_\rho \end{aligned} \quad (13)$$

Where: The state vector $x \in R^n$; The control inputs vector $u \in R^{nu}$; The measurement outputs $y \in R^{ny}$; The controlled outputs $z \in R^{nz}$; The exogenous

inputs (i.e. disturbances) $w \in R^{nw}$, z_ρ and $w_\rho \in R^r$ are the inputs and outputs of parameter block Θ, with: $\Theta = diag(\rho_1 I_{r1}, \rho_2 I_{r2} \dots \rho_k I_{rk})$.

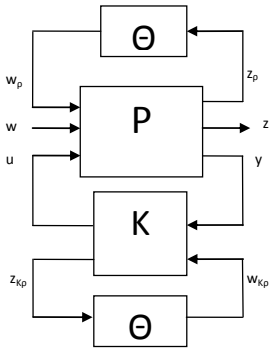

Fig. 4 LFT-LPV closed loop structure

The controller *K(ρ)* is also an LPV system with LFT representation, we present its state space as follows:

$$\begin{aligned} \dot{x}_K &= A_K x_K + B_{K1} y + B_{K\rho} w_{K\rho} \\ u &= C_{K1} x_K + D_{K11} y + D_{K1\rho} w_{K\rho} \\ z_{K\rho} &= C_{K\rho} x_K + D_{K\rho 1} y + D_{K\rho\rho} w_{K\rho} \\ w_{K\rho} &= \Theta z_{K\rho} \end{aligned} \quad (14)$$

Where: $x_K \in R^n$ the controller states vector, $y \in R^{ny}$ the measurement outputs from the plant, $u \in R^{nu}$ the controller outputs, $z_{K\rho}$ and $w_{K\rho} \in R^r$ are inputs and outputs of the parameter block.

We interconnect the inverted pendulum system (7)-(8) with the exogenous inputs (disturbance on the input, measurement noise on the output), we notice in (8), the output matrix ($\mathcal{C}_1 = [1 \quad 0 \quad 0]$) because we consider the angle θ as the only output to stabilize.

As a last step of the designing the closed loop scheme, we provide the applied force (*F*) from the generated input (*u*), from (6):

$$F = u - Ml \sin(\theta)\dot{\theta}^2 \quad (15)$$

The closed-loop scheme is presented in Fig. 5, there are two exogenous inputs (*d*: disturbance, *n*: noise), the measurement output is the error, the only input is the force *F* and we have two controlled outputs (z_e and z_u) which present the performance. Because we have four varying parameters (Table 2), so, z_ρ, w_ρ, $z_{K\rho}$ and $w_{K\rho} \in R^4$.

As we noticed previously, to design the controller, we have to introduce the weighting functions' parameters. Our contribution is based on the choice of the weighting functions' parameters by two evolutionary algorithms (GA and ES) to get the optimal desired performance and as a consequence a robust scheduled controller which guarantees this performance. Next subsection, we show the optimization procedure.

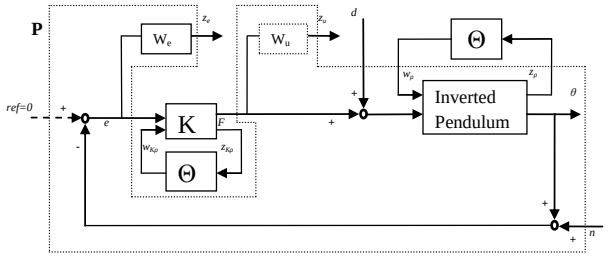

Fig. 5 Closed loop plant-controller interconnection

4.2 The optimization procedure

The optimization tools, GA as well as ES need to specify some characteristics. The weighting functions formula has been taken as a first order filter, the performance criteria has been presented by W_e and W_u (Fig. 5).

$$W_e = k_e \frac{\tau_{e1} s + 1}{\tau_{e2} s + 1} \quad (16)$$

$$W_u = k_u \frac{\tau_{u1} s + 1}{\tau_{u2} s + 1} \quad (17)$$

Therefore, each solution contains six parameters;

$$sol. = [k_e \ \tau_{e1} \ \tau_{e2} \ k_u \ \tau_{u1} \ \tau_{u2}] \quad (18)$$

The main effect of the optimization by the evolutionary algorithms is the multi-objective optimization. We have taken two dynamical indices, settling time, *ST(θ(t))*, and the overshoot, *OV(θ(t))*. The fitness is as follows:

$$Fitness = 0.3\, ST(\theta(t)) + 0.7\, OV(\theta(t)) \quad (19)$$

The controller synthesis algorithm is achieved by the small gain theorem via LMI conditions, the same algorithm we used in [12], the approach is developed in [11], [28] and we are helped by an LPV toolbox, *LPVTools* [29].

As we noticed, the optimization problem has been achieved by two algorithms (GA and ES), *Algorithm 3* presents the optimization algorithm. We note *Algorithm_i* to mean *Algorithm 1* and *Algorithm 2*, because we use the both of them to solve the same problem. The details of their procedures and characteristics are mentioned in Section 3 and Table 3.

***Algorithm 3** : Optimal weighting functions*
Initialize a solutions (18) randomly;
While** max_Generation not meet **do
Generate the closed loop (Fig. 5);
Design the own controller;
Evaluate the solutions based on fitness(19)
Replace the solutions based on Algorithm_i;

end while

The optimal parameters which are obtained by GA and ES, are presented in Table 4. Thanks to the optimization algorithms, we guarantee the low pass filter of the control, on both of algorithms, because the H∞ guarantees this condition $\left|\frac{K}{1+KP}\right| \leq \left|\frac{1}{W_u}\right|$, where *K* is the controller, *P* is the plant [1].

Table 4 weighting functions parameters

Parameter	k_e	τ_{e1}	τ_{e2}	k_u	τ_{u1}	τ_{u2}
LPV-GA	3.28	4.01	6.60	0.67	6.36	0.24
LPV-ES	6.16	7.49	2.72	1.09	5.96	0.64
[12]	5	0.04	1	1	1	0.1

4.3 Simulation results

We get an LFT-LPV H_∞ controller with weighting functions selection by GA optimization and another by ES. The fitness function was a combination between settling time and overshoot of the angle's signal, the controller guarantees the robustness against the disturbances and noises. Fig. 6 presents a comparison of the dynamic response between the obtained controller with GA (*LPV-GA*), the one obtained with ES (*LPV-ES*), and the one of the previous work [12]. The weighting functions, in [12], were selected by *trial-and-error*. no disturbance neither noise are applied, the initial angle is 60°,.

In Fig. 6, we notice that the angle stabilization is done with the three controllers, but, the response has less settling time in *LPV-GA* and *LPV-ES* (less than *1 s*), unlike the settling time of [12] curve. In the other criteria, the overshoot, in *LPV-GA* curve, and [12] curve, the overshoot reach *-4*°, it is smaller than that in *LPV-ES* which is *-6*°. Between these three approaches, we note that the optimal performance is gotten by the weighting functions selected by GA.

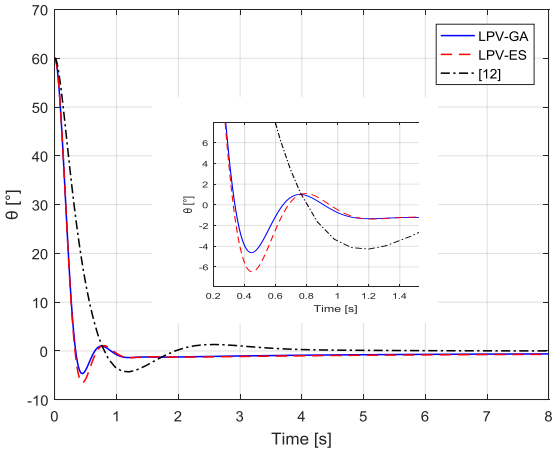

Fig. 6 Dynamic response comparison between LPV_GA, LPV_ES and [12]

Now we pass to another point; the robustness against the exogenous inputs, the external inputs we choose is the input disturbance and the noise, as shown in Fig. 5. We apply a permanent noise between ± *2*°. Starting from *5 s*, we apply a disturbance force of *10 N*, as shown in Fig. 7.

Remark 1: *In the simulation, we won't apply the robust LPV controller on the approximated LPV model (7)-(8) but, on the original nonlinear model itself (4).*

Fig. 8 presents, a simulation of *15 s* and a comparison of the angle response (*θ*) and the linear velocity (*V*) between *LPV-GA* and *LPV-ES* with presence of disturbance and noises (Fig. 7). In the curve of (*θ*) we notice that, there is robustness against the noises, we notice that there is a variation in *5 s* because of the sudden applied force in *5 s*, but ultimately the disturbance is rejected.

We conclude in the last of this section, the nature-inspired optimization tools, GA and ES, effect on the weighting functions selection. In addition to getting an optimal performance, the scheduled controller, LFT-LPV, guarantees the robustness against the external signals. But, the linear velocity (*V*) do never reach the null (the vehicle doesn't stop) because we are not caring of it in the controller design and the system is considered as a Single Input Single Output system (SISO). This is what we are discussing in the next section.

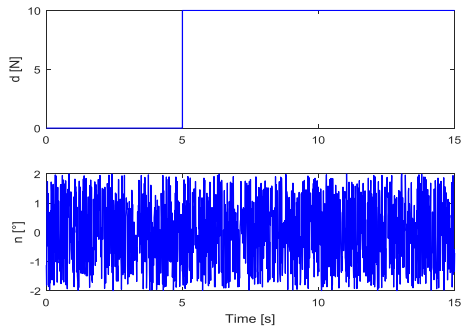

Fig. 7 The disturbance and the noise

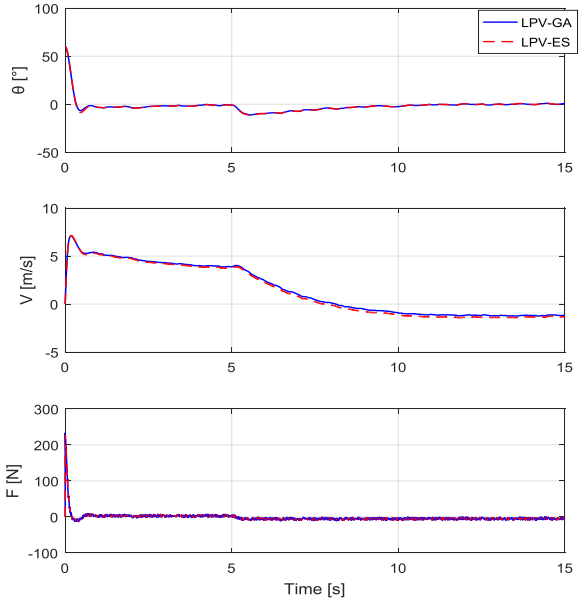

Fig. 8 The angle (θ), the velocity (V) and the force (F) responses with presence of disturbance and noise

5 Extended LPV stabilization to the 2DOF

An underactuated mechanical system (UMS) is a system that has fewer control inputs than the degrees of freedom, as well as the inverted pendulum, which has two degrees of freedom, one is relating on translational coordinate (x), and the other is relating rotational coordinate (θ), but just one control input, the force (F). In the previous section, the inverted pendulum has been stabilized by a robust LPV H_∞ controller, but, by considering it as a SISO system. In the previous simulation (Section 4), the velocity reaches the null very slowly (300 seconds).

The underactuation may impose a constraint; we have to take this constraint into account. May some scientists say; alternatively to consider the angle (θ) the only output, we consider tow outputs; the angle (θ) and the linear velocity ($\dot{\theta}$) and generate its suitable LPV controller.

In fact, we tried to control the inverted pendulum as a general Single-Input-Multi-Outputs system (SIMO), we changed the output matrix of (7) by ($c_1 = \begin{bmatrix} 1 & 0 & 0 \\ 0 & 0 & 1 \end{bmatrix}$), the response, either the angle or the velocity is oscillation and never stabilize (Fig. 9). The weighting functions are obtained by GA.

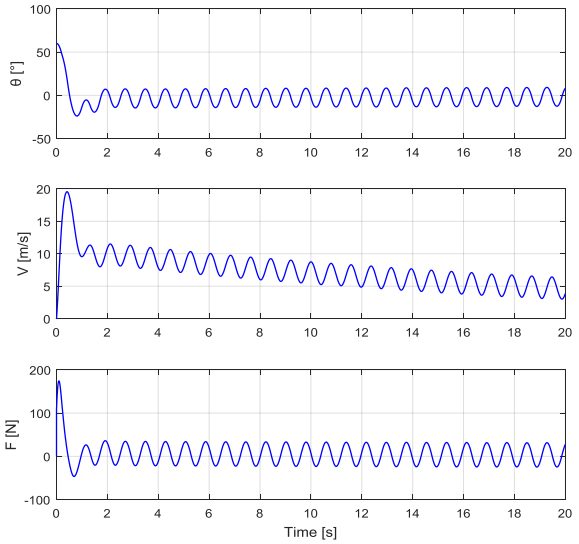

Fig. 9 The dynamic response of the inverted pendulum as a SIMO system

In literature, there is no unique methodology to control a UMS, there are different classifications. One of the most common is *Seto and Baillieul* classification. It is depending on the so-called Control Flow Diagram (CFD). According to this classification, a UMS could have a chain structure, tree structure or isolated-vertex structure, for more detail see; [30], [31].

The inverted pendulum is under the tree class. There are subclasses into the tree structure (A1, A2) [31]. Since the first (A1) could be converted to a chain class by changing the states and controlled as a chain structure by Backstepping [32]. The other subclass (A2) could not, in [33], the authors proposed a method; the configuration variables (the degrees of freedom) of the system should be controlled simultaneously; we have to include in the control law, some terms related to stabilize the angle (θ) and some terms related to stabilize the linear velocity ($\dot{\theta}$). We will denote to the state $\dot{\theta}$,by v.

The only expression has information about (θ) is the error (the measurement output of the LPV plant, Fig. 5), the closed loop system has been changed by adding proportional term related to (v), k_v v (Fig. 10), the gain k_v presents the weight of the velocity, we choose k_v=*0.02*. The new output is (θ + *0.02* v).

Remark 2*: In this stage, we didn't design another controller, but we kept the controller we designed in Section 4.*

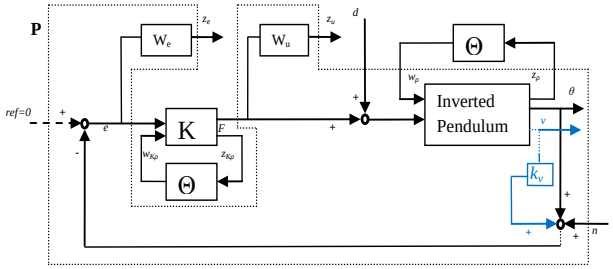

Fig. 10 Underactuated closed loop plant-controller

We pass now to the simulation phase, Fig. 11 presents the dynamic response of the angle (θ), the velocity (V) and the force (F) of the both controllers (*LPV-GA* and *LPV-ES*), with the presence of disturbance and noise as well as presented in Fig. 7, we notice that, in addition to control of the angle, the velocity is controlled and it has been ultimately reaches to zero, on the both of curves (*LPV-GA* and *LPV-ES*). The overshoot exceeds (-20°), that what the pendulum needs to balance the pendulum. We note also that, the system is robust against the permanent noise, and the disturbance is rejected.

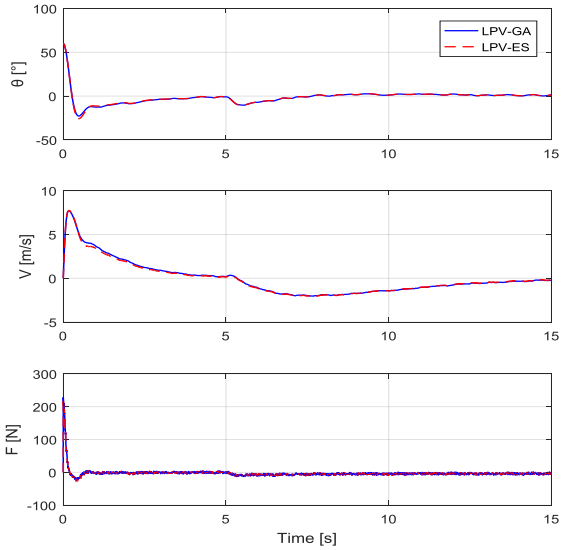

Fig. 11 The angle (θ), the velocity (V) and the force (F) responses with adding the velocity term

One important point on the robust control, when the H_∞ controller is achieved, it is so guaranteed the worst case of uncertainties. That means, the closed-loop system is asymptotically stable for any $\|\Delta\|_\infty \leqslant 1$.

Remark 3*: the stability of the augmented system is robust (plant-weighting functions), so, the performance of the system is robust because the performance is presented by the weighting functions.*

In our system, the pendulum's mass presents the mass of the rider, we can apply the uncertainty according the rider's mass, we took *70 Kg* as a nominal mass (Table 1), in the next simulation figures, we took *M=nominal value ± 43%* (*40 Kg*, *70 Kg* and *100 Kg*). Fig. 12 presents the response with uncertainty of *LPV-GA*. Fig. 13 presents the response with uncertainty of *LPV-ES*. We note that the controllers are robust against the uncertainty, the angular overshoot is between -20° and -30°, the peak velocity is *8 m/s* when (*M=100*), *9 m/s* when (*M=70*) and *10 m/s* when (*M=40*).

All of the previous simulations are achieved with 60° as an initial angle. Next, the simulation results of the dynamic responses are achieved with different initial angles (60°, 30°, -30° and -60°). Fig. 14 presents the dynamic responses of *LPV-GA*, Fig. 15 presents the dynamic responses of *LPV-ES*. On the both of controllers, the 2DOF are controlled; the angle and the velocity reach the equilibrium point simultaneously; in addition it is robust whatever the initial angle.

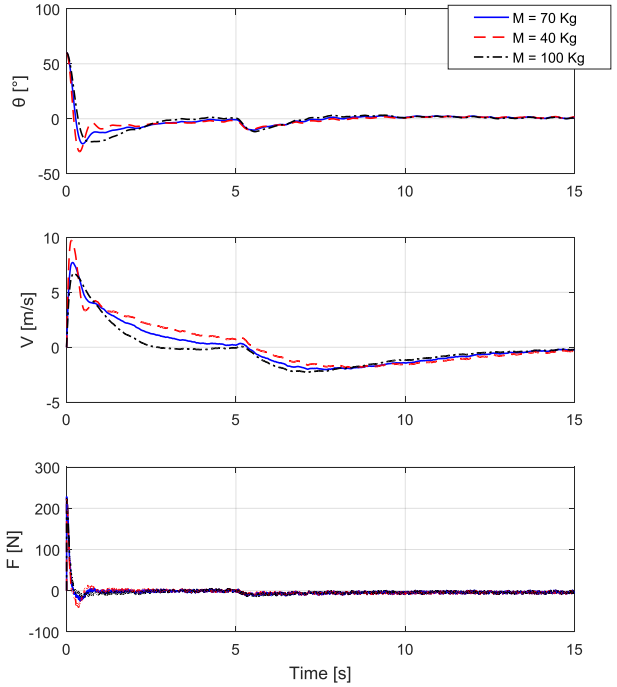

Fig. 12 The angle (θ), the velocity (V) and the force (F) responses with uncertainty on *LPV-GA*

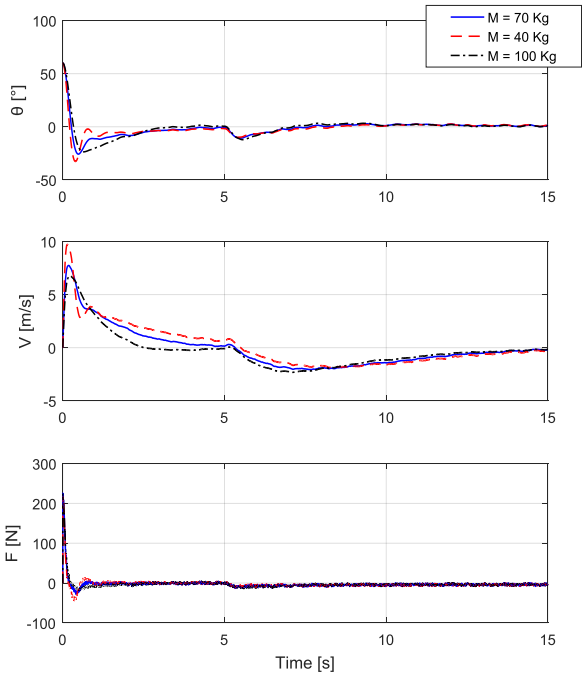

Fig. 13 The angle (θ), the velocity (V) and the force (F) responses with uncertainty on *LPV-ES*

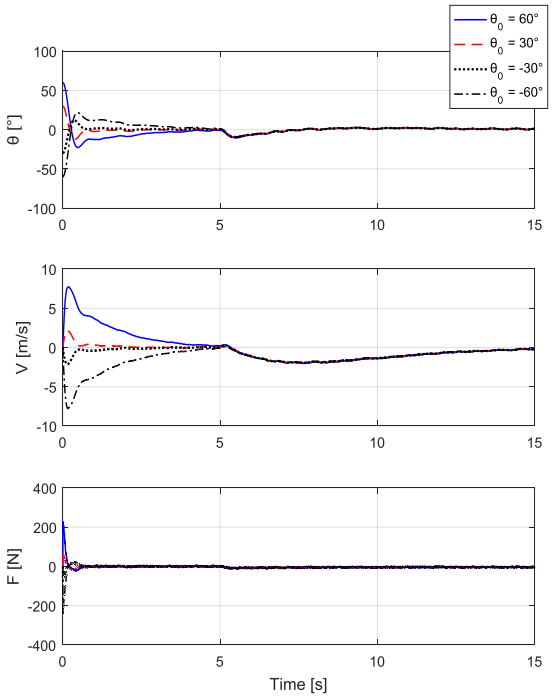

Fig. 14 The angle (θ), the velocity (V) and the force (F) responses with different initial angles on *LPV-GA*

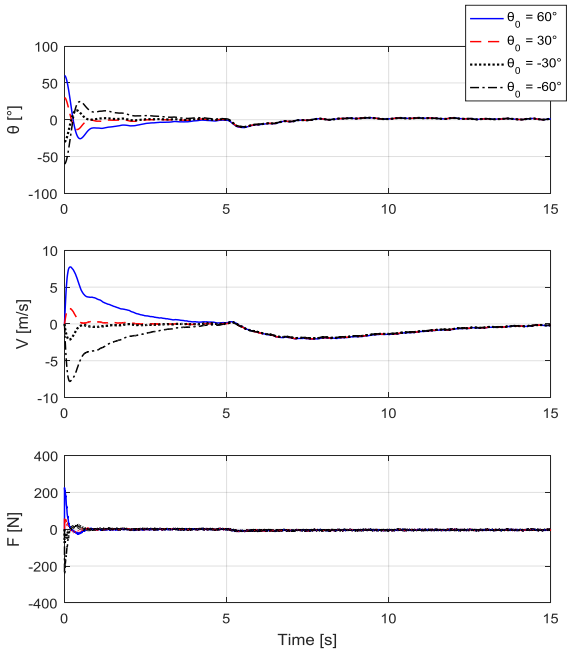

Fig. 15 The angle (θ), the velocity (V) and the force (F) responses with different initial angles on *LPV-ES*

6 Conclusion

In this paper, the robust stabilization problem of the inverted pendulum on cart is considered. We applied a scheduled robust controller with type

LFT-LPV H_∞. As a first step we created its nonlinear model as an LPV system with LFT representation. Second, we were interesting on the weighting functions parameters selection; we suggested solving it by two nature-inspired optimization algorithms (GA and ES). Thanks to those, in addition to get an optimal performance, the robustness is guaranteed against the perturbations and the uncertainties. Last and important point we investigated, is the underactuation problem. The inverted pendulum imposes this constraint. Our objective is to balance the inverted pendulum, where its angle and velocity be zero, without adding another actuator. After we modify the closed loop structure, the simulation results showed an optimal obtained performance, the objective is successfully done. It is robust against the external signals and uncertainties.

References:

[1] K. Zho, and J. C. Doyle, *Essentials of Robust Control*, Prentice Hall, Upper Saddle River, NJ, 1998.

[2] T. Iwasaki, and G. Shibata, LPV system analysis via quadratic separator for uncertain implicit system, *IEEE Transactions on Automatic Control*, Vol. 46, No. 10, 2001, pp. 1195-1208.

[3] C. W. Scherer, LPV control and full block multipliers, *Automatica*, Vol. 37, No. 3, 2001, pp. 361-375.

[4] F. Wu, A generalized LPV system analysis and control synthesis framework, *International Journal of Control*, Vol. 74, No. 9, 2001, pp. 745-759.

[5] J. Shamma, and M. Athans, Gain scheduling: potential hazards and possible remedies, In: *American Control Conference*, Boston, USA, 1991, pp. 516-521.

[6] H. S. Abbas, R. Tóth, M. Petreczky, N. Meskin, and J. Mohammadpour, Embedding of nonlinear systems in a Linear Parameter-Varying representation, In: *IFAC World Congress*, Cape Town, South Africa, 2014, pp. 6907-6913.

[7] G. Balas, J. Bokor, and Z. Szabo, Invariant subspaces for LPV systems and their applications, *IEEE Transactions on Automatic Control*, Vol. 48, No. 13, 2003, pp. 2065-2069.

[8] S. Salhi, N. Aouani, and S. Salhi, LPV affine modeling, analysis and simulation of DFIG based wind energy conversion system, In: *International Conference on Modelling, Identification and Control*, Sousse, Tunisia, 2015.

[9] Z. Liu, D. Theilliol, F. Gu, Y. He, L. Yang, and J. Han, State feedback controller design for affine parameter-dependent LPV systems, *IFAC PapersOnLine*, Vol. 50, No. 1, 2017, pp. 9760-9765.

[10] F. Wu, X. Yang, A. Packard, and G. Becker, Induced L_2 norm control for LPV systems with bounded parameter variation rates, *International Journal of Robust and Nonlinear Control*, Vol. 6, No. 9-10, 1996, pp. 983-998.

[11] A. Packard, Gain scheduling via linear fractional transformations, *Systems and Control Letters*, Vol. 22, No. 2, 1994, pp. 79-92.

[12] S. Hasseni, and L. Abdou, Robust LPV control applied to a personal pendulum vehicle, In: *International Conference on Sciences and Techniques of Automatic Control and Computer Engineering*, Monastir, Tunisia, 2017, pp. 6-11.

[13] R. W. Beaven, M. T. Wright, and D. R. Seaward, Weighting function selection in the H_∞ design process, *Control Engineering Practice*, Vol. 4, No. 7, 1996, pp. 625-633.

[14] J. Hu, C. Bohn, and H. R. Wu, Systematic H_∞ weighting function selection and its application to the real-time control of a vertical take-off aircraft, *Control Engineering Practice*, Vol. 8, No. 3, 2000, pp. 241-252.

[15] E. Alfaro-Cid, E. W. McGookin, and D. J. Murray-Smith, Optimisation of the weighting function of an H_∞ controller using genetic algorithms and structured genetic algorithms, *International Journal of Systems Science*, Vol. 39, No. 4, 2008, pp. 335-347.

[16] A. L. Do, O. Sename, L. Dugard, and B. Soualmi, Multi-objective optimization by genetic algorithms in H_∞/LPV control of semi-active suspension, In: *IFAC World Congress*, Milano, Italy, 2011, pp. 7162-7167.

[17] V. T. Vu, O. Sename, L. Dugard, and P. Gaspar, Multi objective H_∞ active-roll bar control for heavy vehicles, *IFAC PapersOnLine*, Vol. 50, No. 1, 2017, pp. 13802-13807.

[18] J. H. Holland, *Adaptation in Natural and Artificial Systems*, MIT Press, MA, USA, 1992.

[19] I. Rechenberg, *Evolutionstrategie: Optimieruna Technischer Systeme nach Prinzipien der Biologischen Evolution*, Frommann-Holzboog-Verlag, Stuttgart, Germany, 1973.

[20] M. Fiacchini, A. Viguria, R. Cano, A. Prieto, F. R. Rubio, J. Aracil, and C. Canudas-de-Wit, Design and experimentation of a personal pendulum vehicle, In: *Portuguese Conference on Automatic Control*, Lisbona, Portugal, 2006.

[21] K.C. Schwab, L. Schräder, P. Mercorelli, and J.T. Lassen, Control of the Inverse Pendulum Based on Sliding Mode and Model Predictive Control, *WSEAS Transactions on Systems and Control*, Vol. 13, 2018, pp. 529-536.

[22] G. V. Raffo, M. G. Ortega, and F. R. Rubio, Nonlinear H_∞ Control Applied to the Personal Pendulum Car, In: *European Control Conference*, Kos, Greece, 2007, pp. 2065-2070.

[23] A. Wright, *Genetic Algorithms for Real Parameter Optimization*, Morgan Kaufmann, San Mateo, California, USA, 1991.

[24] L. Abdou, and F. Soltani, OS-CFAR and CMLD threshold optimization with genetic algorithms, In: *International Conference on Systems, Signals & Devices, Vol III Communication and Signal Processing*, Sousse, Tunisia, 2005.

[25] B. K. Yeo, and Y. Lu, Array failure correction with a genetic algorithm, *IEEE Transactions on Antennas and Propagation*, Vol. 47, No. 7, 1999, pp. 823-828.

[26] N. Hansen, D. V. Arnold, and A. Auger, Evolution Strategies. In: *Springer Handbook of Computational Intelligence*, Springer, Heidelberg, Germany, 2015, pp. 871-898.

[27] L. Abdou, and F. Soltani, OS-CFAR and CMLD threshold optimization in distributed systems using evolotionary strategies, *Signal, Image and Video Processing*, Vol. 2, No. 2, 2008, pp. 155-167.

[28] P. Apkarian, and P. Gahinet, A convex characterization of gain-scheduled H_∞ controller, *IEEE Transactions on Automatic Control*, Vol. 40, No. 7, 1995, pp. 853-864.

[29] A. Hjartarson, P. Seiler, and A. Packard, LPV Tools: a toolbox for modeling, analysis and synthesis of parameter varying control systems, *IFAC PapersOnLine*, Vol. 48, No. 26, 2015, pp.136-145.

[30] D. Seto, and J. Baillieul, Control problem in super-articulated mechanical systems, *IEEE Transactions on Automatic Control*, Vol. 39, No. 14, 1994, pp. 2442-2453.

[31] A. Choukchou-Braham, B. Cherki, M. Djemaï, and K. Busawon, Classification of Underactuated Mechanical Systems, In: *Analysis and Control of Underactuated Mechanical Systems*, Springer, London, UK, 2014, pp. 35-54.

[32] S. Rudra, R. K. Barai, and M. Maitra, Block Backstepping Control of the Underactuated Mechanical Systems, In: *Block Backstepping Design of Nonlinear State Feedback Control Law for Underactuated Mechanical Systems*, Springer-Verlag, Singapore, 2017, pp. 31-52.

[33] A. Choukchou-Braham, B. Cherki, M. Djemaï, K. Busawon, Control Design Schemes for Underactuated Mechanical Systems, In: *Analysis and Control of Underactuated Mechanical Systems*, Springer, London, UK, 2014, pp. 55-91.